2015 Tenth International Conference on Ecological Vehicles and Renewable Energies (EVER)

Overview of the Requirements and Implementations of Bidirectional Isolated AC–DC Converters for Automotive Battery Charging Applications

Georgios E. Sfakianakis, *Student Member, IEEE,* Jordi Everts, *Member, IEEE,*
and Elena A. Lomonova, *Senior Member, IEEE*

Electromechanics and Power Electronics (EPE) group
Department of Electrical Engineering
Eindhoven University of Technology (TU/e)
Eindhoven, The Netherlands
g.e.sfakianakis@tue.nl

***Abstract*—This paper is divided into three main parts. In the first part, i.e. Section II, a general outline of the system level aspects regarding battery chargers (power converters) for plug-in electric vehicles (PEVs) is given. Thereby, the different charging modes of the converters, the corresponding power levels, and the infrastructural facilities are discussed. Moreover, Vehicle-to-Grid (V2G) operation by means of grid-forming, grid-feeding, and grid-supporting converter functionality is briefly explained, and the input power quality and electromagnetic compatibility requirements are summarized. In the second part, i.e. Section III, the mutually coupled indices that determine the overall performance of the system, such as power losses (efficiency), volume (power density), weight (specific power), failure rate (reliability), and costs (relative cost), are outlined. In this context, the role that wide band-gap power semiconductors (e.g. SiC, GaN) can play in order to further improve the system performance is highlighted. In the third part, i.e. Section IV, a concise overview of the possible topological implementations for the mentioned power converters is provided. The focus is on conductive, isolated AC–DC converter topologies with high AC input power quality in terms of power factor correction (PFC) and harmonic distortion, and with bidirectional power flow capability in order to facilitate V2G operation.**

***Index Terms*—Bidirectional Isolated AC–DC Converters, Battery Chargers, Conductive Charging, Plug-in Electric Vehicles**

I. Introduction

The number of plug-in hybrid electric vehicles (PHEVs) and battery electric vehicles (PBEVs), hereafter generally denoted as plug-in electric vehicles (PEVs), has constantly been increasing during the past years [1]. Due to their superior fuel economy and performance compared to internal combustion engine vehicles (ICEVs), they can effectively contribute to a lower environmental impact of the ever-increasing use of personal vehicles [2].

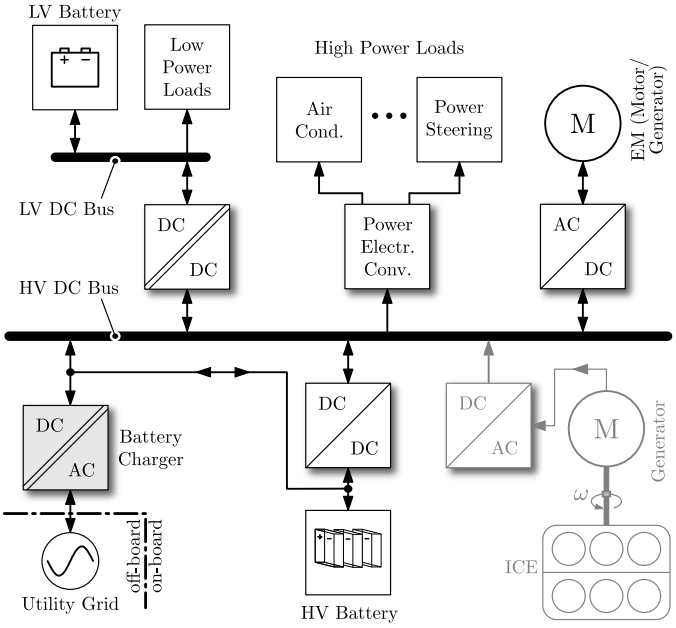

Fig. 1. Typical PBEV electric power system architecture [3]. The PBEV turns into a PHEV in case an internal combustion engine present (gray colored part).

978-1-4673-6785-1/15/$31.00 ©2015 European Union

Figure 1 shows a typical electric power system architecture of a pure-electric PBEV, comprising an electric machine (EM) which draws energy from a high voltage (HV) battery during propulsion, and recharges the battery during regenerative braking. For the case at hand, both the EM and the HV battery are connected to a HV DC bus[1] via a bidirectional, non-isolated AC–DC and DC–DC power electronic converter respectively. Also connected to the HV DC bus via power converters are the high power loads, such as the air conditioning and the power streering, and a low voltage (LV, typically $14\ \mathrm{V_{DC}}$) DC bus for providing energy to the low power loads (e.g. lightning, instrumentation, pumps, etc.). When adding an internal combustion engine (ICE) and electric generator to the power system, connecting them to the HV DC bus via an AC–DC rectifier as shown by the gray colored part in Figure 1, the PBEV turns into a series PHEV.

For all types of PEVs, the HV battery can be externally recharged by plugging into the low voltage utility grid using different types of conductive or inductive battery chargers. The charger shown in Figure 1 is an on-board, conductive, single-phase AC–DC converter which can either be directly connected to the HV battery or to the HV DC bus (case at hand). At first, i.e. in Section II of this paper, an overview of all standardized battery charger options is given by means of the so called 'charging modes', the corresponding power levels, and the infrastructural facilities. PEV battery chargers can also be distinguished by their capability to manage unidirectional or bidirectional power flow. The class of bidirectional converters is becoming more attractive as besides charging of the HV battery, they can also transfer energy from the battery to the grid in order to provide Vehicle-to-Grid (V2G) services. The features of grid-forming, grid-feeding, and grid-supporting V2G operation are discussed in Section II as well. Lastly, the AC input power quality and electromagnetic compatibility requirements for battery chargers are summarized.

In the design of power electronic converters, especially in automotive applications, there is a historical trend toward lower losses, volume, weight, failure rate, and costs [2]. These indices that determine the overall performance of the system, as well as their mutual coupling, are outlined in Section III. In this context, the role that wide band-gap power semiconductors (e.g. SiC, GaN) can play in order to further improve the system performance is also highlighted, along with the importance of thermal management. Since multiple objectives need to be considered for the design of a power electronic converter, the necessity of multi-objective optimization (MOO) of converter systems is described too.

In Section IV of this paper, a concise overview of the possible topological implementations for conductive AC–DC converters is given. The topologies are classified into two families: single-stage and two-stage architectures. The focus is on single-phase and three-phase converters with high AC input power quality in terms of power factor correction (PFC) and harmonic distortion, and with bidirectional power flow capability in order to facilitate V2G operation. Only topologies with galvanic isolation are considered since they are seen as a favorable option in conductive chargers[2] [5].

II. Battery Chargers: System Level Aspects

A. Charging Modes

Battery chargers for PEVs can be subdivided into two main categories: conductive and inductive chargers [5]. As far as it concerns the *conductive chargers*, power is transfered through metal-to-metal contact between the connector on the charging port of the vehicle and the AC power lines, or a dedicated electric vehicle supply equipment (EVSE) that is interfaced with the AC utility grid. Thereby the required AC–DC power conversion can either take place within the PEV utilizing an on-board charger, or within the EVSE involving an off-board charger. For the latter, DC power is fed to the vehicle through a cable. This method is also known as 'DC charging', enabling higher charging current/power and thus smaller charging times. The international standard IEC 61851-1 [4] was created by the International Electrotechnical Commission (IEC) in order to provide a framework that applies to on-board and off-board conductive charging equipment for PEVs, inter alia defining requirements regarding the cable connection between the PEV and the charging point, the types of plugs and sockets, and the corresponding safety measures and communication features [6], [7]. Most relevant for this overview are the different charging modes, which mainly relate to the current and power levels of the chargers:

- **Mode 1 charging (on-board); Figure 2(a):** slow charging whereby energy is sourced from the AC

[1] Voltage levels of $200\ \mathrm{V_{DC}}$ to $400\ \mathrm{V_{DC}}$, and even up to $650\ \mathrm{V_{DC}}$ for the HV DC bus are rather common [2].

[2] Besides increased safety, galvanic isolation provides more convenience to fulfill the requirements given in the standards [4]. For example, in non-isolated chargers, the presence of common-mode currents, noise, and so on, requires a considerable effort to prevent unwanted earth fault protection trip [5].

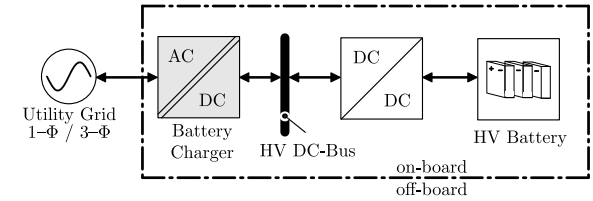

(a) Mode 1 and mode 2 charging

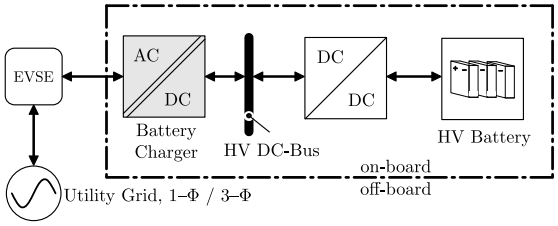

(b) Mode 3 charging

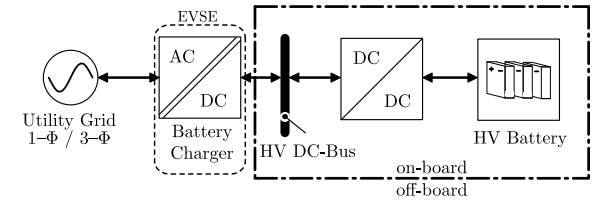

(c) Mode 4 (DC) charging

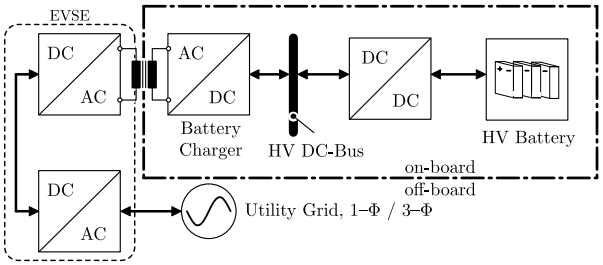

(d) Inductive charging

Fig. 2. Charging infrastructure for conductive (a)-(c) and inductive (d) charging. Note that the DC output of the battery chargers might also be directly connected to the terminals of the HV battery.

grid utilizing a typical single-phase or three-phase household-type socket. The charging current is limited to 16 $\mathrm{A_{AC}}$, while the AC voltage may not exceed 250 $\mathrm{V_{AC}}$ for a single-phase, and 480 $\mathrm{V_{AC}}$ for a three-phase supply outlet. The IEC-recommended AC voltage is $230/400$ $\mathrm{V_{AC}}$, resulting in a maximum charging power of 3.7 kW (single-phase) and 11 kW (three-phase) [6], [7].

- **Mode 2 charging (on-board); Figure 2(a):** slow charging from a household-type socket with an in-cable protection device. The voltage ratings are the same as for mode 1, but the maximum current is 32 $\mathrm{A_{AC}}$. Thus, the achievable charging power is 7.4 kW (single-phase) and 22 kW (three-phase) [6], [7].
- **Mode 3 charging (on-board); Figure 2(b):** slow or fast charging using dedicated EVSE, involving a PEV socket outlet with control, protection function, and other additional safety features installed. Charging currents up to 63 $\mathrm{A_{AC}}$ are allowed. The maximum power level is thus 14.5 kW (single-phase) and 43.5 kW (three-phase). Very high AC charging currents up to 250 $\mathrm{A_{AC}}$ are also described by the standard [4], [6], [7].
- **Mode 4 charging (off-board); Figure 2(c):** fast DC-current charging, with charging currents up to 400 $\mathrm{A_{DC}}$ that are provided by an off-board charger which is located within the EVSE.

For *inductive chargers*, the power is transfered via a magnetic coupling (wireless, see Figure 2(d)) [8]. This technology offers galvanic isolation, connector robustness, power compatibility, durability, and a user friendly interface. However, these advantages come at a cost of a low conversion efficiency and the need for new, costly charging infrastructure [5]. A separate international standard, SAE-J2954, is currently being prepared by the Society of Automotive Engineers (SAE), concerning the alignment of the vehicle as well as the infrastructure needed. Inductive battery chargers are not further discussed.

B. Vehicle-to-Grid (V2G) Operation

Conventional unidirectional battery chargers can only absorb power from the utility grid in order to charge the batteries. Recently, the concept of Vehicle-to-Grid (V2G) operation has gained an increasing interest as an opportunity to improve the efficiency and reliability of the grid by providing grid support services. Thereby, energy stored in the batteries of the total fleet of PEVs that are parked and connected to the grid can be injected into the grid, enabling for example the implementation of peak shaving, voltage control, and the integration of more renewable energy sources. Evidently this requires bidirectional power electronic converters. The role that these grid-connected converters can play in providing ancillary services depends on how they are designed and operated [9], [10]:

- **Grid-forming** converters (see Figure 3(a)) are represented as an ideal voltage source with low output impedance [9]. They are controlled to generate a voltage with given amplitude and frequency. An example of a grid-forming converter is a standby uninterruptible power supply (UPS), where in case of grid failure the UPS converter forms the grid.

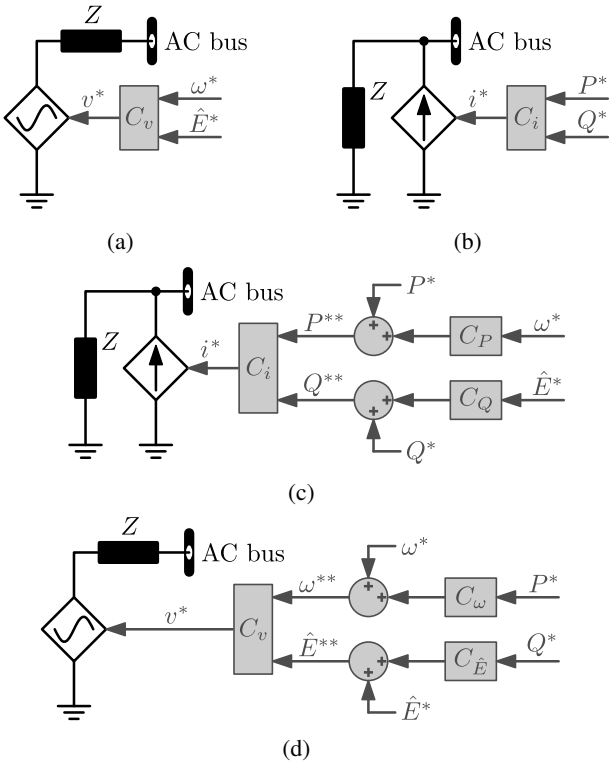

Fig. 3. Simplified representation of grid-connected power converters [9]. (a) Grid-forming, (b) grid-feeding, (c) grid-supporting (current-source-based), and (d) grid-supporting (voltage-source-based).

- **Grid-Feeding** converters (see Figure 3(b)) are represented as an ideal current source with high parallel impedance [9]. They are controlled to deliver a certain amount of active and reactive power to an energized grid. Grid-forming converters cannot operate in island mode.
- **Grid-Supporting** converters (see Figures 3(c) and 3(d)) are represented as either a current source with parallel impedance (Figure 3(c)) or a voltage source with a link impedance (Figure 3(d)) [9]. Their active and reactive power are controlled to contribute to the regulation of the grid voltage and frequency. The current source implementation does need an energized grid to operate while the voltage source implementation does not.

C. Standards of Operation

1) AC Input Power Quality: The quality of the AC input power can be quantified using both the power factor and the amount of harmonic current injection into the grid. For single-phase and three-phase converters rated less than 16 $\mathrm{A_{AC}}$ per phase, which include mode 1 chargers, IEC has created an international standard known as IEC 61000-3-2 [11]. Thereby, electrical devices are divided into 4 classes according to their power and application. Battery chargers are classified in Class A, where the low-frequency harmonics of the mains current should not exceed the values listed in Table I. For converters rated greater than 16 $\mathrm{A_{AC}}$ per phase (which include mode 2, 3, and 4 chargers) and that are intended to be connected to public low-voltage AC distribution systems, the IEC 61000-3-4 standard [12] applies, defining limits to the low-frequency harmonics of the mains current in a similar way as IEC 61000-3-2. Additionally, the IEEE has created a guide [13] which is applicable to single-phase converters rated less than 600 $\mathrm{V_{AC}}$ and 40 $\mathrm{A_{AC}}$. It is suggested that the maximum total harmonic distortion (THD) of the current should be less than 15%, and that the 3$^{\mathrm{rd}}$ current harmonic should be less than 10% of the fundamental current component, while the power factor should not be less than 0.95. For lower power devices, the maximum allowed values are doubled to 30% for the THD of the current and to 20% of the fundamental for the 3$^{\mathrm{rd}}$ current harmonic.

TABLE I
LIMITS FOR CLASS A EQUIPMENT [11]

Harmonic order n	Maximum permissible harmonic current (A)
Odd harmonics	
3	2.30
5	1.14
7	0.77
9	0.40
11	0.33
13	0.21
$15 \leqslant n \leqslant 39$	$2.25/n$
Even harmonics	
2	1.08
4	0.43
6	0.30
$8 \leqslant n \leqslant 40$	$1.84/n$

2) Electromagnetic Compatibility (EMC): The high levels of switched currents and voltages can be seen as the main characteristics of a power converter [14]. As a result of this characteristic, power converters generate electromagnetic fields/emission which are guided through conductors (conducted emission; 150 kHz - 30 MHz) or air (radiated emission; 30 MHz - 1 GHz), and which potentially lead to electromagnetic interference (EMI). Therefore, the IEC has created the International Special Committee on Radio Interference–CISPR, defining standards in order to ensure electromagntic compatibility (EMC) of converter systems that are to be commercialized. The CISPR 11 [15] and CISPR 22 [16]

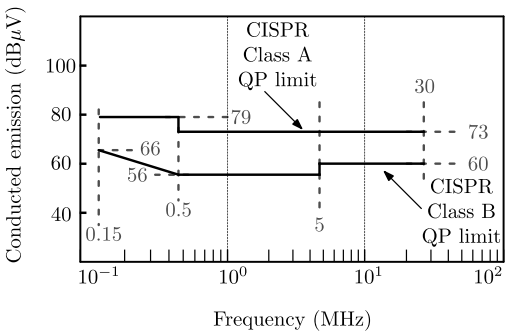

Fig. 4. Quasi-peak limits for conducted emissions at the main ports of Class A and Class B equipment according to CISPR 11 and 22.

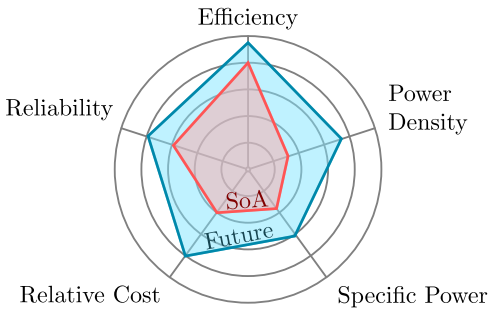

Fig. 5. A spider graph illustrating the State of the Art (SoA) and future expected performance indices of a power electronic converter system.

have been created for Class A (residential) and Class B (light industrial) equipment. Common for both CISPR 11 and CISPR 22 are the quasi-peak limits for conducted emissions which are shown in Figure 4 for both Class A and B equipment.

Although efforts have been put on the study of the impact of modulation schemes and soft-switching techniques on *conducted emissions*, filtering circuits that effectively limit the propagation of electrical noise can not be avoided [14]. In [17], for example, a design procedures has been proposed for the optimal design of these filter circuits. Thereby, the switching frequency should be selected carefully in order to minimize the impact on the power density and efficiency, and to maximize the dynamic response [18]. *Radiated emissions*, on the other hand, are typically reduced and controlled by development of good layout techniques and shielding [14].

III. Converter Performance

A. Performance Indices

The main quantities that determine the performance of a power electronic converter are the power losses, the volume, the weight, the failure rate, and the system costs [19]. In order to assess and compare different converters, and in order to define a plan of action for the further development of converter systems, these mutually coupled factors can be expressed by relative quantities that are termed 'performance indices', being respectively the efficiency, power density, specific power, reliability, and relative costs. Their continuous enlargement is one of the main design objectives for future (on-board) PEV battery chargers. This is illustrated in Figure 5, while a summary of the performance indices is presented below.

1) Power Losses (Efficiency): Due to environmental reasons and in connection with rising energy prices, the efficiency of converter systems is gaining more importance. The efficiency of a converter is defined as:

$$\eta = 100 \cdot \frac{P_\mathrm{o}}{P_\mathrm{i}} \qquad [\%]\,, \tag{1}$$

where P_o is the output power and P_i the input power. Efficiency is directly related to power losses, where three main sources of them can be distinguished: power semiconductors, passive components and auxiliary components. The power semiconductor part of the losses can be split in two parts, the switching and the conduction losses. Regarding switching losses, a trade-off is introduced since by increasing the switching frequency, in order to reduce the size of passive components, the switching losses are increased. However, by means of soft-switching techniques such as zero voltage switching (ZVS) or zero current switching (ZCS), the switching of the semiconductors with quasi-zero switching losses is achieved. Furthermore, passive components (inductors, capacitors) used for filtering and energy transfer, consume quite a lot of energy which can reach almost 20% of the total losses [18]. Auxiliary losses consist of losses related to the power supply of the cooling system, the digital control, and the power semiconductor drivers. It should be noted that an increased efficiency also results in reduced cooling requirements and thus a lower weight, volume, and again cost.

2) Volume (Power Density) and Weight (Specific Power): Power density expresses how compact a system is, while specific power can define the nominal power of a converter in respect of weight. Power density ρ and specific power γ are defined as the nominal output power $P_\mathrm{o,nom}$ of the converter divided by its volume V and its

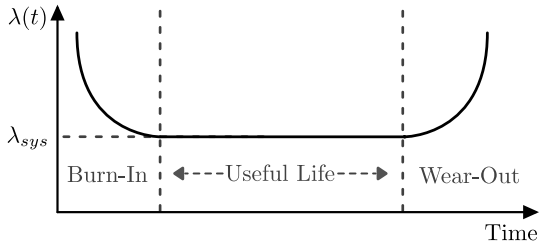

Fig. 6. A typical reliability curve (also known as Bathtub curve), indicating the failure rate of a device during different time intervals of its lifetime.

weight W, respectively:

$$\rho = \frac{P_{\mathrm{o,nom}}}{V} \qquad [\mathrm{kW/liter}, \mathrm{kVA/liter}]\,, \tag{2}$$

$$\gamma = \frac{P_{\mathrm{o,nom}}}{W} \qquad [\mathrm{kW/kg}, \mathrm{kVA/kg}]\,. \tag{3}$$

A low converter weight and volume enable simple handling, installation, and maintenance of the system [2]. In case no thermal limitations apply, this can be achieved by increasing the switching frequency, resulting in smaller passive components like transformers, capacitors and inductors, and thus again in lower weight and cost [2]. Note that a reduced weight also results in a driving range expansion of the vehicles. However, as mentioned above, an increased switching frequency comes at the cost of higher power losses.

3) Failure Rate (Reliability): The reliability is the ability of a system or component to perform its required functions under stated conditions for a specified period of time [20]. A quantitative measure to determine the reliability is the failure rate λ, i.e. the availability of an item after an elapsed time. A typical failure rate curve is illustrated in Figure 6, which is know as the bathtub curve. Three main periods can be distinguished: the burn-in, the useful life, and the wear-out period. The useful life of a battery charger, as part of a PEV, should be close to the lifetime of the vehicle. This will further increase the penetration of PEVs into the market. However, in order to increase the reliability of the system, typically more components are required [20], which might result in decreased performance of other attributes (e.g. power density, specific power, cost), requiring a trade-off analysis.

4) System Cost (Relative Cost): By providing cheaper solutions for battery chargers and propulsion systems, the integration of PEVs into vehicle market can be accelerated. A quantitative measure to define the overall system cost is the 'relative cost' performance index:

$$\sigma = \frac{P_{\mathrm{o,nom}}}{C} \qquad [\mathrm{kW/\$}, \mathrm{kVA/\$}, \mathrm{kW/€}, \mathrm{kVA/€}]\,, \tag{4}$$

which expresses the nominal power divided by the total cost of the system. Furthermore, an important figure is the time needed for a technology to be available in the market, known as 'time to market'. For example, despite the fact that first attempts of realization of Silicon Carbide (SiC) power semiconductors were reported in the 1990s [21], the first commercially available SiC JFET switch was only recently introduced in the market [22].

B. The Role of Wide Band-Gap Devices

Wide band-gap semiconductors such as Gallium Nitride (GaN) and Silicon Carbide (SiC) are to play a key role in the advancement of power electronic switching devices and thus converters [23]–[25]. The advantages of wide band-gap materials compared to Silicon, whereof the performance is close to its physical limits [23], are their high-voltage blocking capability, low on-state resistance, high switching speed, and high-temperature operation. The latter is due to the small intrinsic carrier densities. Experiments with GaN and SiC transistors have proved a stable operation at $300\ ^{\circ}\mathrm{C}$ and $450\ ^{\circ}\mathrm{C}$ respectively, while silicon transistors achieve stable operation at temperatures up to $150\ ^{\circ}\mathrm{C}$ [26], [27]. Moreover, switching frequencies of a few hundred kilohertz in hard-switching operation are feasible [28], [29], while for Si devices this is only possible by employing soft-switching strategies. In [30] efficiencies exceeding 99.5% have been reported, utilizing SiC JFET devices in an inverter application. This could be achieved due to the low voltage drop across the devices (i.e. small on-resistance), resulting in low conduction losses, and due to the short switching time, leading to low switching losses. To conclude, wide band-gap devices form an new era in power electronics, which might be the enabler of ultra-high performance power converters systems.

C. The Role of Multi-Objective Optimization (MOO)

In the design of power electronic systems, the trend is to minimize the volume and maximize the available power. Moreover, general requirements are also applied for cost minimization and lifetime increase, while environmental issues highlight efficiency maximization as a major concern. As a result, multiple objectives should be considered, which are the minimization of the volume, the weight, the losses, the cost as well as the failure rate. As mentioned before, these objectives are translated

into measurable 'Performance Indices' and based on them, quantitative assessments are possible. Therefore the process of optimization of a system requires to take into account more objectives and a mathematical procedure (MOO) is required to assure the best possible exploitation of the available degrees of freedom and technologies [19].

The mathematical MOO procedure maps a multi-dimensional Design Space (Decision Space) into a multi-dimensional Performance Space (Objective Space), which is defined by the different Performance indices p_i, as illustrated in Figure 7.

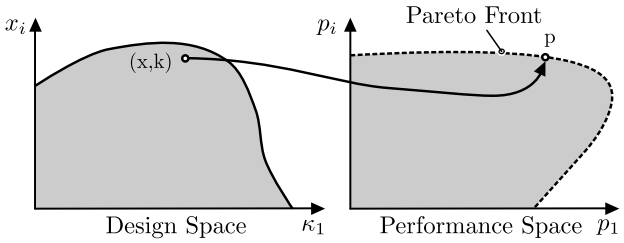

Fig. 7. Qualitative representation of the Design Space (left) and Performance Space (right), illustrating a random mapping of a design decision (x,k) to the corresponding performance. The boundary of the Performance Space is defined by the pareto front which represents the best possible performance of the power electronics system.

IV. AC–DC Converter Topologies

In this section a concise overview of the possible topological implementations for conductive battery chargers which can be used for mode 1, mode 2, mode 3, and mode 4 charging (acc. to Section II-A) is presented. The focus is on single-phase and three-phase AC–DC converters with high AC input power quality in terms of power factor correction (PFC) and harmonic distortion, and with bidirectional power flow capability in order to facilitate V2G operation (see Section II-B). As explained in the introduction (see Section I), only topologies with galvanic isolation are considered. Assuming that each converter is made up of a set of building blocks as shown in Figure 8, the topologies are classified into two families: single-stage and dual-stage architectures.

A. Dual-Stage AC–DC Converter Topologies

As shown in Figure 8(a), dual-stage bidirectional and isolated AC–DC converters are most commonly realized using a power factor correction (PFC) converter followed by an isolated DC–DC converter, being both bidirectional. The PFC performs the rectification of the AC line voltage into a DC voltage that might be boosted to a higher level. The PFC also must assure the quality

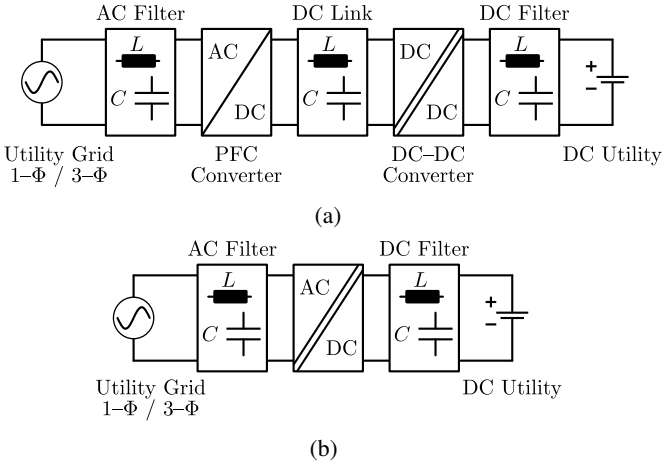

Fig. 8. General representation of (a) dual-stage AC–DC converter topologies and (b) single-stage AC–DC converter topologies.

of the AC input power in terms of power factor and harmonic distortion. In addition, an AC filter is present at the AC side in order to filter the high-frequency harmonic components of the AC input current. The DC output side of the PFC converter is connected to a DC-link storage element which can be an inductor (current DC-link) or a capacitor (voltage DC-link). The later is used more often and therefore considered only in this paper. The smoothed DC-link voltage (or current) is further inputted to the isolated DC–DC converter, providing power to the DC facility (e.g. the HV DC bus or the HV battery of the car). Dual-stage converters have the advantage that the PFC stage and the isolated DC–DC conversion stage are decoupled via the DC energy storage element. Consequently, both systems can be optimized within narrow specifications.

1) PFC Converter Topologies: The most widespread way to implement bidirectional PFC front-ends is to use pulse-width-modulated bridge circuits that interface the DC-link storage capacitor (voltage DC-link) with the mains [31]–[33]. Thereby, one or more bulky line inductors are typically present. Figures 9(a) and 9(b) respectively show a *single-phase* half-bridge and full-bridge PFC, while Figure 9(c) shows a *three-phase* full-bridge variant. The line inductors are useful to suppress the current harmonics injected into the grid by the PWM voltage that is impressed at the AC terminals of the PFC converter. However, an additional AC filter section is generally required to comply with the standards.

In [33] and [34], an extensive review of the *single-phase*, boost-type PFC front-end converters, such as the ones shown in Figures 9(a) and 9(b), is presented, along with some other variants such as multi-level (e.g. neutral

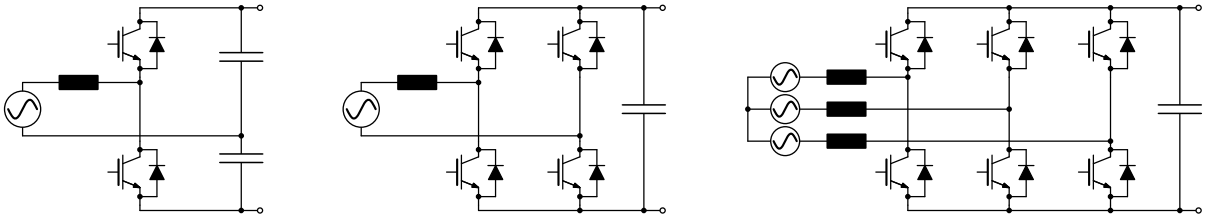

Fig. 9. Bidirectional PFC AC–DC converter topologies based on conventional bridge circuits. (a) Single-phase half-bridge converter, (b) single-phase full-bridge converter, and (c) three-phase full-bridge converter.

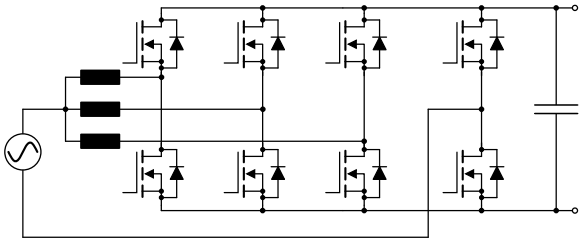

Fig. 10. Single-phase, bidirectional, multi-cell, totem-pole PFC AC–DC converter.

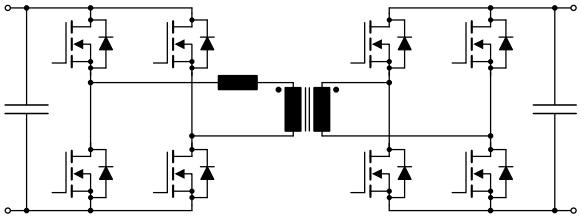

Fig. 11. Isolated, bidirectional, full-bridge full-bridge DAB DC–DC converter.

point clamped (NPC) or T-type), buck-type, and buck-boost-type architectures. Furthermore, a bidirectional multi-cell totem-pole PFC converter (acc. to Figure 10) is described in [35], [36], employing a triangular current mode (TCM) soft-switching modulation scheme over the complete mains period.

In [37], a comparative evaluation of the two-level *three-phase*, boost-type PFC front-end converter shown in Figure 9(c) and the three-level NPC variant of this converter is presented. Reference [38] presents a comparative evaluation of *three-phase*, buck-type, bidirectional PFC converters based on conventional unidirectional rectifier topologies that are modified using an inverting link-circuit. Besides the unidirectional six-switch PFC system and the anti-parallel six-switch converter, also topologies based on the 3rd harmonic injection concept such as the bidirectional SWISS converter [39] are investigated.

2) Isolated DC–DC Converter Topologies: Numerous different types of isolated DC–DC converter topologies are proposed in literature, such inter alia the soft-switching dual active bridge (DAB) topologies and the resonant topologies, whether or not combined with active auxiliary snubber circuits and/or a second non-isolated DC–DC conversion stage. Extensive overviews, topology surveys, and comparative evaluations are presented in [40]–[44]. Figure 11 shows the full-bridge full-bridge DAB implementation which, amongst other variants, is considered as the most suitable candidate for the realization of high-efficiency, high-power density, isolated DC–DC conversions [42].

B. Single-Stage AC–DC Converter Topologies

Besides the traditional dual-stage approach, bidirectional and isolated AC–DC converters with PFC can also be realized using a single power conversion stage. These single-stage AC–DC converters are identified by the absence of an intermediate DC-link storage element and can be referred to as matrix-type converters. Due to the effective omission of a complete power conversion stage and DC-link energy storage element they have the potential to benefit the system performance with regard to efficiency, volume (power density), number of components (reliability), weight, and costs [2]. For single-phase converters this comes at the cost of an increased filtering effort on the DC side in order to reduce the low-frequency output ripple due to the power variation at the double line frequency. This deficiency vanishes for three-phase architectures which only require storage at the switching frequency in case of symmetrical sinusoidal current consumption. Another deficiency of the single-stage converters is that all converter functionalities such as the PFC, the galvanic isolation, the suppression of the line frequency harmonics, and the output voltage regulation are performed by a single conversion stage that consequently needs to be designed and optimized within wide specifications.

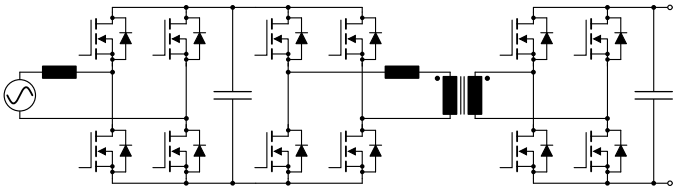

Fig. 12. Single-stage, single-phase, bidirectional, isolated, soft-switched AC–DC converter based on the full-bridge full-bridge DAB.

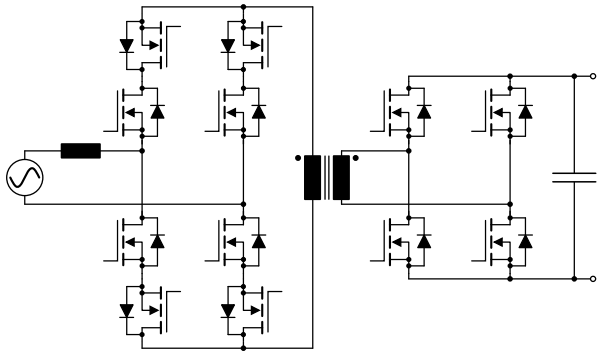

Fig. 13. Single-stage, single-phase, bidirectional, isolated, soft-switched AC–DC converter, using a cycloconverter on the AC side, a voltage-source converter on the DC side, and a medium frequency transformer in between.

Different types of single-stage, *single-phase*, bidirectional, and isolated AC–DC converters have been proposed in literature, such as the true bridgeless PFC converter [45] and different variants of the single-stage DAB AC–DC converter topologies [46]–[52], which use matrix-type 'low-frequency AC to high-frequency AC' modules at the AC side. A very promising variant is the single-stage full-bridge full-bridge DAB AC–DC converter presented in [51]–[53] and shown in Figure 12. It is shown in [53] that this converter can be controlled under soft-switching conditions within its complete operating range. In [54], [55] another single-stage, soft-switched AC–DC converter topology is proposed. This topology is shown in Figure 13, using a cycloconverter on the AC side, a voltage-source converter on the DC side, and a medium frequency transformer in between.

Single-stage, *three-phase*, bidirectional, and isolated AC–DC converters comprise the three-phase DAB [56], and the three-phase soft-switched converter that consists of a cycloconverter and a voltage-source converter [57] (acc. to Figure 14). Another approach based on a stackable multi-port converter is presented in [58] and shown in Figure 15, combining three separate single-phase matrix-type 'low-frequency AC to high-frequency AC' modules using a single transformer structure. As can

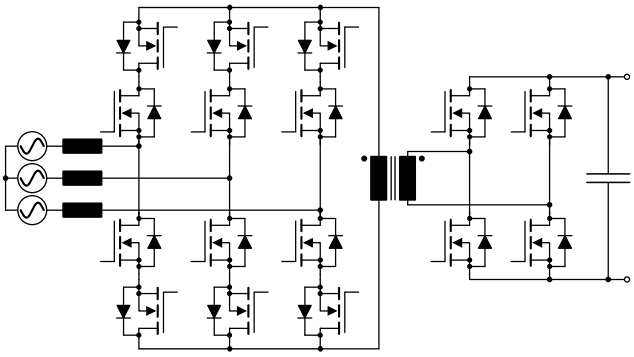

Fig. 14. Single-stage, three-phase, bidirectional, isolated, soft-switched AC–DC converter, using a cycloconverter on the AC side, a voltage-source converter on the DC side, and a medium frequency transformer in between.

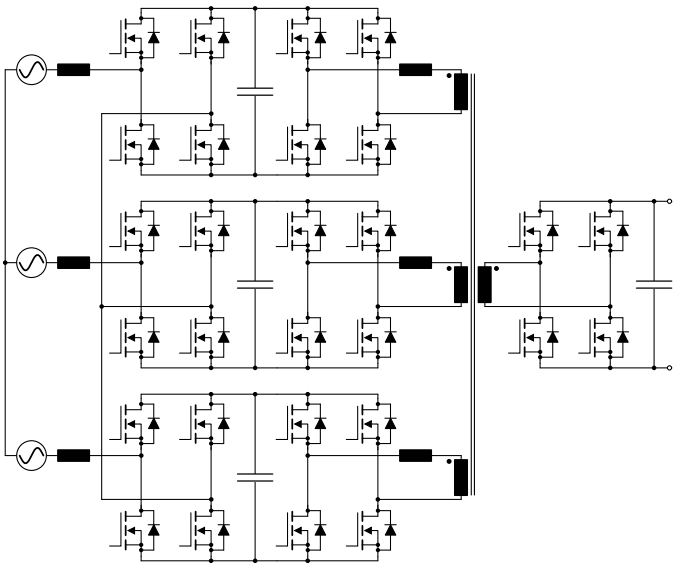

Fig. 15. Single-stage, three-phase, bidirectional, isolated, soft-switched AC–DC converter based on separate single-phase matrix-type 'low-frequency AC to high-frequency AC' modules using a single transformer structure.

be seen from Figure 15, this converter has a close similarity with the single-stage, single-phase DAB converter topology depicted in Figure 12. Besides the advantage of modularity, low voltage semiconductor devices can be used which feature a low on-state resistance and fast switching behavior. Additionally, the converter can be controlled with a modulation scheme that facilitates soft-switching operation.

V. Conclusion

In this paper the requirements and the implementations of bidirectional isolated AC–DC converters for automotive battery charging applications have been overviewed and different aspects have been discussed into three

main parts. In the first part, a general outline of the system level aspects regarding battery chargers for PEVs is given. Furthermore, Vehicle-to-Grid (V2G) operation is briefly explained while the input power quality and electromagnetic compatibility requirements are outlined. In the second part, the mutually coupled indices that determine the overall performance of the system, such as power losses (efficiency), volume (power density), weight (specific power), failure rate (reliability), and costs (relative cost), are summarized. The role that wide band-gap power semiconductors (e.g. SiC, GaN) can play in order to further improve the system performance is highlighted, as well as the role of Multi-Objective Optimization (MOO). In the last part, a brief overview of the possible topological implementations for the mentioned power converters is provided. The focus is on conductive, isolated AC–DC converter topologies with high AC input power quality in terms of power factor correction (PFC) and harmonic distortion, and with bidirectional power flow capability in order to facilitate V2G operation.

ACKNOWLEDGMENTS

This paper is part of the ADvanced Electric Powertrain Technology (ADEPT) project which is an EU funded Marie Curie ITN project, grant number 607361. Within ADEPT a virtual and hardware tool are created to assist the design and analysis of future electric propulsions. Especially within the context of the paradigm shift from fuel powered combustion engines to alternative energy sources (e.g. fuel cells, solar cells, and batteries) in vehicles like motorbikes, cars, trucks, boats, planes. The design of these high performance, low cost and clean propulsion systems has stipulated an international cooperation of multiple disciplines such as physics, mathematics, electrical engineering, mechanical engineering and specialisms like control engineering and safety. By cooperation of these disciplines in a structured way, the ADEPT program provides a virtual research lab community from labs of European universities and industries [59].

REFERENCES

[1] C. C. Chan, "The State of the Art of Electric, Hybrid, and Fuel Cell Vehicles," *Proceedings of the IEEE*, vol. 95, no. 4, pp. 704–718, April 2007.

[2] J. Everts, "Modeling and Optimization of Bidirectional Dual Active Bridge AC–DC Converter Topologies," Ph.D. dissertation, University of Leuven (KU Leuven), Leuven, Belgium, 2014.

[3] A. Emadi, K. Rajashekara, S. S. Williamson, and S. M. Lukic, "Topological Overview of Hybrid Electric and Fuel Cell Vehicular Power System Architectures and Configurations," *IEEE Transactions on Vehicular Technology*, vol. 54, no. 3, pp. 763–770, May 2005.

[4] IEC 61851-1, "Electric Vehicle Conductive Charging System – Part 1: General Requirements." IEC, International Electrotechnical Commission, Geneva, Switzerland, 2001.

[5] S. Haghbin, S. Lundmark, M. Alakula, and O. Carlson, "Grid-Connected Integrated Battery Chargers in Vehicle Applications: Review and New Solution," *IEEE Transactions on Industrial Electronics*, vol. 60, no. 2, pp. 459–473, Feb. 2013.

[6] S. Luyten, N. Leemput, F. Geth, J. Van Roy, J. Büscher, and J. Driesen, "Standardization of Conductive AC Charging Infrastructure for Electric Vehicles," in *22nd International Conference on Electricity Distribution (CIRED 2013)*, June 2013, Paper 0476.

[7] A. Mathoy (BRUSA Elektronic). (2008) Definition and Implementation of a Global EV Charging Infrastructure (Last accessed: 23/07/2013). [Online]. Available: http://www.park-charge.ch/documents/EV-infrastructure%20project.pdf

[8] M. G. Egan, D. L. O'Sullivan, J. G. Hayes, M. J. Willers, and C. P. Henze, "Power-Factor-Corrected Single-Stage Inductive Charger for Electric Vehicle Batteries," *IEEE Transactions on Industrial Electronics*, vol. 54, no. 2, pp. 1217–1226, April 2007.

[9] J. Rocabert, A. Luna, F. Blaabjerg, and P. Rodriguez, "Control of Power Converters in AC Microgrids," *IEEE Transactions on Power Electronics*, vol. 27, no. 11, pp. 4734–4749, Nov. 2012.

[10] Li, Y W and Kao, C.-N., "An Accurate Power Control Strategy for Power-Electronics-Interfaced Distributed Generation Units Operating in a Low-Voltage Multibus Microgrid," *IEEE Transactions on Power Electronics*, vol. 24, no. 12, pp. 2977–2988, Dec. 2009.

[11] IEC 61000-3-2, "Electromagnetic Compatibility (EMC) – Part 3-2: Limits for Harmonic Current Emissions (Equipment Input Current $\leqslant$ 16 A per Phase)." IEC, International Electrotechnical Commission, Geneva, Switzerland, 1995.

[12] IEC 61000-3-4, "Electromagnetic compatibility (EMC) – Part 3-4: Limitation of Emission of Harmonic Currents in Low-Voltage Power Supply Systems for Equipment with Rated Current Greater than 16 A." IEC, International Electrotechnical Commission, Geneva, Switzerland, 1998.

[13] "IEEE Draft Guide for Applying Harmonic Limits on Power Systems," *IEEE P519.1/D12*, pp. 1–124, July 2012.

[14] M. L. Heldwein, "EMC Filtering of Three-Phase PWM Converters," Ph.D. dissertation, Swiss Federal Institute of Technology (ETH Zürich), Power Electronic Systems (PES) Laboratory, Zürich, Switzerland, 2008.

[15] C.I.S.P.R., "Specification for Industrial, Scientific and Medical (ISM) Radio-Frequency Equipment - Electromagnetic Disturbance Characteristics - Limits and Methods of Measurement – Publication 11." IEC, International Special Committee on Radio Interference, Geneva, Switzerland, 2004.

[16] ——, "Limits and Methods of Measurement of Radio Disturbance Characteristics of Information Technology Equipment–Publication 22." IEC, International Special Committee on Radio Interference, Geneva, Switzerland, 1993.

[17] T. Nussbaumer, M. L. Heldwein, and J. W. Kolar, "Differential Mode Input Filter Design for a Three-Phase Buck-Type PWM Rectifier Based on Modeling of the EMC Test Receiver," *IEEE Transactions on Industrial Electronics*, vol. 53, no. 5, pp. 1649–1661, Oct. 2006.

[18] J. W. Kolar, F. Krismer, Y. Lobsiger, J. Muhlethaler, T. Nussbaumer, and J. Minibock, "Extreme Efficiency Power Electronics," in *7th International Conference on Integrated Power Electronics Systems (CIPS 2012)*, March 2012, pp. 1–22.

[19] J. W. Kolar, J. Biela, S. Waffler, T. Friedli, and U. Badstuebner, "Performance Trends and Limitations of Power Electronic Systems," in *6th International Conference on Integrated Power Electronics Systems (CIPS 2010)*, March 2010, pp. 1–20.

[20] Y. Song and B. Wang, "Survey on Reliability of Power Electronic Systems," *IEEE Transactions on Power Electronics*, vol. 28, no. 1, pp. 591–604, Jan. 2013.

[21] G. Kelner, M. S. Shur, S. Binari, K. J. Sleger, and H. S. Kong, "High-Transconductance β–SiC Buried-Gate JFETs," *IEEE Transactions on Electron Devices*, vol. 36, no. 6, pp. 1045–1049, June 1989.

[22] J. Rabkowski, D. Peftitsis, and H. P. Nee, "Silicon Carbide Power Transistors: A New Era in Power Electronics is Initiated," *IEEE Industrial Electronics Magazine*, vol. 6, no. 2, pp. 17–26, June 2012.

[23] J. Everts, J. Das, J. Van den Keybus, M. Germain, and J. Driesen, "GaN-Based Power Transistors for Future Power Electronic Converters," in *Proceedings of the IEEE Benelux Young Researchers Symposium on Smart Sustainable Power Delivery (YRS 2010)*, March 2010.

[24] J. Rabkowski, D. Peftitsis, and H. P. Nee, "Silicon Carbide Power Transistors: A New Era in Power Electronics is Initiated," *IEEE Industrial Electronics Magazine*, vol. 6, no. 2, pp. 17–26, June 2012.

[25] J. Millan and P. Godignon, "Wide Band Gap Power Semiconductor Devices," in *IEEE Spanish Conference on Electron Devices (CDE 2013)*, Feb. 2013, pp. 293–296.

[26] L. F. Eastman and U. K. Mishra, "The Toughest Transistor Yet [GaN Transistors]," *IEEE Spectrum*, vol. 39, no. 5, pp. 28–33, May 2002.

[27] P. G. Neudeck, R. S. Okojie, and L.-Y. Chen, "High-Temperature Electronics - a Role for Wide Bandgap Semiconductors?" *Proceedings of the IEEE*, vol. 90, no. 6, pp. 1065–1076, June 2002.

[28] J. S. Glaser, J. J. Nasadoski, P. A. Losee, A. S. Kashyap, K. S. Matocha, J. L. Garrett, and L. D. Stevanovic, "Direct Comparison of Silicon and Silicon Carbide Power Transistors in High-Frequency Hard-Switched Applications," in *IEEE 26th Annual Applied Power Electronics Conference and Exposition (APEC 2011)*, March 2011, pp. 1049–1056.

[29] J. Biela, M. Schweizer, S. Waffler, and J. W. Kolar, "SiC versus Si – Evaluation of Potentials for Performance Improvement of Inverter and DC–DC Converter Systems by SiC Power Semiconductors," *IEEE Transactions on Industrial Electronics*, vol. 58, no. 7, pp. 2872–2882, July 2011.

[30] J. Rabkowski, D. Peftitsis, and H. P. Nee, "Design Steps Toward a 40-kVA SiC JFET Inverter With Natural-Convection Cooling and an Efficiency Exceeding 99.5%," *IEEE Transactions on Industry Applications*, vol. 49, no. 4, pp. 1589–1598, July 2013.

[31] M. Bertoluzzo, N. Zabihi, and G. Buja, "Overview on Battery Chargers for Plug-In Electric Vehicles," in *IEEE 15th International Power Electronics and Motion Control Conference (EPE/PEMC 2012)*, Sept. 2012, pp. LS4d.1–1 – LS4d.1–7.

[32] M. Yilmaz and P. T. Krein, "Review of Battery Charger Topologies, Charging Power Levels, and Infrastructure for Plug-In Electric and Hybrid Vehicles," *IEEE Transactions on Power Electronics*, vol. 28, no. 5, pp. 2151–2169, May 2013.

[33] B. Singh, B. N. Singh, A. Chandra, K. Al-Haddad, A. Pandey, and D. P. Kothari, "A Review of Single-Phase Improved Power Quality AC-DC Converters," *IEEE Transactions on Industrial Electronics*, vol. 50, no. 5, pp. 962–981, Oct. 2003.

[34] J. P. M. Figueiredo, F. L. Tofoli, and B. L. A. Silva, "A Review of Single-Phase PFC Topologies Based on the Boost Converter," in *IEEE/IAS 9th International Conference on Industry Applications (INDUSCON 2010)*, Nov. 2010, pp. 1–6.

[35] C. Marxgut, J. Biela, and J. W. Kolar, "Interleaved Triangular Current Mode (TCM) Resonant Transition, Single Phase PFC Rectifier with High Efficiency and High Power Density," in *International Power Electronics Conference (IPEC 2010)*, June 2010, pp. 1725–1732.

[36] C. Marxgut, F. Krismer, D. Bortis, and J. W. Kolar, "Ultraflat Interleaved Triangular Current Mode (TCM) Single-Phase PFC Rectifier," *IEEE Transactions on Power Electronics*, vol. 29, no. 2, pp. 873–882, Feb. 2014.

[37] J. Moia, J. Lago, A. J. Perin, and M. L. Heldwein, "Comparison of Three-Phase PWM Rectifiers to Interface AC Grids and Bipolar DC Active Distribution Networks," in *IEEE 3rd International Symposium on Power Electronics for Distributed Generation Systems (PEDG 2012)*, June 2012, pp. 221–228.

[38] M. F. Vancu, T. Soeiro, J. Muhlethaler, J. W. Kolar, and D. Aggeler, "Comparative Evaluation of Bidirectional Buck-Type PFC Converter Systems for Interfacing Residential DC Distribution Systems to the Smart Grid," in *IEEE 38th Annual Conference on Industrial Electronics Society (IECON 2012)*, Oct. 2012, pp. 5153–5160.

[39] T. B. Soeiro, T. Friedli, and J. W. Kolar, "SWISS Rectifier – A Novel Three-Phase Buck-Type PFC Topology for Electric Vehicle Battery Charging," in *IEEE 27th Annual Applied Power Electronics Conference and Exposition (APEC 2012)*, Feb. 2012, pp. 2617–2624.

[40] R. L. Steigerwald, "A Comparison of Half-Bridge Resonant Converter Topologies," *IEEE Transactions on Power Electronics*, vol. 3, no. 2, pp. 174–182, April 1988.

[41] R. L. Steigerwald, R. W. De Doncker, and M. H. Kheraluwala, "A Comparison of High-Power DC–DC Soft-Switched Converter Topologies," *IEEE Transactions on Industry Applications*, vol. 32, no. 5, pp. 1139–1145, Sept.-Oct. 1996.

[42] F. Krismer, J. Biela, and J. W. Kolar, "A Comparative Evaluation of Isolated Bi-directional DC/DC Converters with Wide Input and Output Voltage Range," in *40th Industry Applications Conference Annual Meeting (IAS 2005)*.

[43] A. Mehdipour and S. Farhangi, "Comparison of Three Isolated Bi-Directional DC/DC Converter Topologies for a Backup Photovoltaic Application," in *2nd International Conference on Electric Power and Energy Conversion Systems (EPECS 2011)*, Nov. 2011, pp. 1–5.

[44] N. M. L. Tan, T. Abe, and H. Akagi, "Topology and Application of Bidirectional Isolated DC–DC Converters," in *IEEE 8th International Conference on Power Electronics and ECCE Asia (ICPE 2011 - ECCE Asia)*, May 2011, pp. 1039–1046.

[45] S. Cuk, "True Bridgeless PFC Converter Achieves Over 98% Efficiency, 0.999 Power Factor," *Power Electronics Technology Magazine*, Part 1: pp. 10–18, July 2010; Part 2: pp. 34–40, Aug. 2010; Part 3: pp. 22–31, Oct. 2010.

[46] K. Vangen, T. Melaa, S. Bergsmark, and R. Nilsen, "Efficient High-Frequency Soft-Switched Power Converter with Signal Processor Control," in *IEEE 13th International Telecommunications Energy Conference (INTELEC 1991)*, Nov. 1991, pp. 631–639.

[47] M. H. Kheraluwala and R. W. De Doncker, "Single Phase Unity Power Factor Control for Dual Active Bridge Converter," in

IEEE Industry Applications Society Annual Meeting, vol. 2, Oct. 1993, pp. 909–916.

[48] J. Everts, J. Van den Keybus, and J. Driesen, "Switching Control Strategy to Extend the ZVS Operating Range of a Dual Active Bridge AC/DC Converter," in *IEEE Energy Conversion Congress and Exposition (ECCE 2011)*, Sept. 2011, pp. 4107–4114.

[49] J. Everts, J. Van den Keybus, F. Krismer, J. Driesen, and J. W. Kolar, "Switching Control Strategy for Full ZVS Soft-Switching Operation of a Dual Active Bridge AC/DC Converter," in *IEEE 27th Annual Applied Power Electronics Conference and Exposition (APEC 2012)*, Feb. 2012, pp. 1048–1055.

[50] F. Jauch and J. Biela, "Single-Phase Single-Stage Bidirectional Isolated ZVS AC-DC Converter with PFC," in *15th International Power Electronics and Motion Control Conference (EPE/PEMC 2012)*, Sept. 2012, pp. LS5d.1–1–LS5d.1–8.

[51] J. Everts, F. Krismer, J. Van den Keybus, J. Driesen, and J. W. Kolar, "Charge-Based ZVS Soft Switching Analysis of a Single-Stage Dual Active Bridge AC-DC Converter," in *IEEE Energy Conversion Congress and Exposition (ECCE 2013)*, Sept. 2013, pp. 4820–4829.

[52] N. D. Weise, K. Basu, G. Castelino, and N. Mohan, "A Single-Stage Dual Active Bridge Based Soft Switched AC–DC Converter with Open-Loop Power Factor Correction and Other Advanced Features," *IEEE Transactions on Power Electronics*, vol. 29, no. 8, pp. 4007–4016, Aug. 2014.

[53] J. Everts, F. Krismer, J. Van den Keybus, J. Driesen, and J. W. Kolar, "Optimal ZVS Modulation of Single-Phase Single-Stage Bidirectional DAB AC–DC Converters," *IEEE Transactions on Power Electronics*, vol. 29, no. 8, pp. 3954–3970, Aug. 2014.

[54] S. Norrga, "A Soft-Switched Bi-Directional Isolated AC/DC Converter for AC-Fed Railway Propulsion Applications," in *International Conference on Power Electronics, Machines and Drives (PEMD 2002)*, June 2002, pp. 433–438.

[55] ——, "Experimental Study of a Soft-Switched Isolated Bidirectional AC-DC Converter Without Auxiliary Circuit," *IEEE Transactions on Power Electronics*, vol. 21, no. 6, pp. 1580–1587, Nov. 2006.

[56] N. D. Weise, K. Basu, and N. Mohan, "Advanced Modulation Strategy for a Three-Phase AC–DC Dual Active Bridge for V2G," in *IEEE Vehicle Power and Propulsion Conference (VPPC 2011)*, Sept. 2011, pp. 1–6.

[57] S. Norrga, S. Meier, and S. Ostlund, "A Three-Phase Soft-Switched Isolated AC–DC Converter Without Auxiliary Circuit," *IEEE Transactions on Industry Applications*, vol. 44, no. 3, pp. 836–844, May 2008.

[58] F. Jauch and J. Biela, "Modelling and ZVS Control of an Isolated Three-Phase Bidirectional AC-DC Converter," in *IEEE 15th European Conference on Power Electronics and Applications (EPE 2013)*, Sept. 2013, pp. 1–11.

[59] A. Stefanskyi, A. Dziechciarz, F. Chauvicourt, G. E. Sfakianakis, K. Ramakrishnan, K. Niyomsatian, M. Curti, N. Djukic, P. Romanazzi, S. Ayat, S. Wiedemann, W. Peng, and S. Stipetic, "Researchers within the EU funded Marie Curie ITN project ADEPT, grant number 607361," , 2013-2017.